ORIGINAL ARTICLE

GMJ.2017;6(2):136-44
www.gmj.ir

Received 2017-02-08
Revised 2017-05-26
Accepted 2017-05-29

DOI: 10.22086/GMJ.V6I2.822

Preparation and Characterization of Myristoylated Chitosan Nanogel as Carrier of Silibinin for Breast Cancer Therapy

Maliheh Entezari[1]✉, Fereshteh Atabi[2]

[1] Department of Biology, Tehran Medical Sciences Branch, Islamic Azad University, Tehran, Iran
[2] Department of Biochemistry, Tehran Medical Sciences Branch, Islamic Azad University, Tehran, Iran

Abstract

Background: Biopolymer has been known to have compatibility; nontoxic nature and degradation behavior. Chitosan (CS) is being widely used in various biomedical and pharmaceutical applications and serves as a drug carrier. Nanotechnology has emerged as tumor cell target therapy and increase drug bioavailability. One of the most common and important models of cancer in women is breast cancer, which is the fifth most common death reason. Silibinin (SIL) as a flavonolignan, has demonstrated anticancer effects against various human cancer cells, such as breast cancer. **Materials and Methods:** Myristoylated CS (MCS) nanoparticles were prepared on the base of 9:1 ratio related to CS: Myristate and loaded with SIL, for the first time. Then in vitro loading and releasing capacity of nano drug were evaluated. The nanogel structure and its derivatives were characterized by different biophysical methods. The MCF-7 breast cancer cell line and human umbilical vein endothelial cells (HUVEC) cell lines were incubated with 100, 150, and 200µg/ml of SIL and nanoSIL. Afterward cell cytotoxicity was measured by MTT assay. Lethal dose 50 (LD50) or IC50 was measured by Pharm software. **Results**: Compared to HUVEC as normal cells, the proliferation of MCF-7 cells were significantly inhibited ($P<0.01$) by SIL and nano-SIL in a concentration-related manner in defining times ($P<0.05$). SIL-loaded nanogels were more effective than SIL alone ($P<0.01$). The mean size of MCS particles was about 20nm. The MCS nanogels were spheral and homogen with a dense surface. The loading efficiency was obtained about 85-95%. **Conclusions**: It seems the obtained MCS nanogel can play a real and important role as a suitable drug carrier with a high loading capacity to treat cancerous cells with the least side effect. **[GMJ.2017;6(2):136-44] DOI: 10.22086/GMJ.V6I2.822**

Keywords: Chitosan; Myristoylated; Silibinin; Nanogel; Breast Cancer

Introduction

Breast cancer as a most important and universal model of cancer in women that is the fifth most common death reason [1]. Silibinin (SIL) and silymarin as a phytochemical polyphenol are a type of flavonolignan. The main part of the milk thistle seeds (*Silybum Marianum*) consists of SIL. SIL is widely known as a kind of food supplement, mainly in the USA. It is catching the most attention among these antioxidants [2]. In some way, nanotechnology with its increasing explora-

GMJ
©2017 Galen Medical Journal
Tel/Fax: +98 71 36474503
PO Box 7193616563
Email:info@gmj.ir

✉ **Correspondence to:**
Maliheh Entezari, Department of Biology, Tehran Medical Sciences Branch, Islamic Azad University, Tehran, Iran
Telephone Number: +982122006664
Email Address : mentezari@iautmu.ac.ir

tion in different fields of science has made significant progression in biomedical usage such as new technical drug deliveries [3]. There is tremendous interest in a wide range of nanotechnology and polymers in the pharmaceutical industry and therapeutic innovation among with the others [3]. Typically, a drug-loaded in a nanocarrier can protect the drug against degradation or inactivation en route to the target position [4].

Nanoparticle-mediated site-specific targeting approaches also offer an opportunity for using some of the most drugs for disease treatment that otherwise could not be administered due to severe drug-related toxicity problems [5]. There has been considerable research in the development of biodegradable nanoparticles as effective drug delivery systems [5]. Drug immobilization on a proper bed achieved by fixing drugs within supports offers a proper method for stabilizing, storage and sustained release of medications. The drug is dissolved, entrapped, adsorbed, attached or encapsulated into the nanoparticle matrix.

The nanoparticle matrix can be of biodegradable materials such as polymers or proteins [5]. Depending on the method of preparation, nanoparticles can be obtained with different properties, releasing characteristics of the encapsulated therapeutic agents [5]. Recently immobilization techniques have been significantly improved [6]. Parameters such as nanoparticle size, morphology, and chemical makeup can be tailored to the type, developmental stage, and location of a given disease [4]. Nanogels are attractive vehicles for drug scavenging in vivo because of their easy injectability, large surface area-to-volume ratios, and low probability of embolic phenomena [7]. While the loading capacity of the current developer's nanoscale drug carriers toward the drugs is still low, improving the loading efficiency is critical in drug carrier research for effective drug action [8].

Chitosan (CS) as a nanogel is a natural cationic biopolymer (pKa 6.5-7.0) of glucosamine (GlcN) and N-acetylglucosamine (GlcNAc), obtained by partial deacetylation of acetamide groups of chitin [9, 10]. Acetylated and deactivated monomers have been specified to distribute randomly [9, 10].

The average molecular weight of the CS is between 10 and 1000 kDa, and the degree of deacetylation (DD) is usually between 70 and 95% and are dependent on deacetylation conditions [11].

The CS is a natural biodegradable and biocompatible polymer which has been used in controlled drug delivery system [12, 13]. CS is considered non-toxic, with an oral half maximal inhibitory concentration (IC50) over 16 g/kg in mice [5].

It is a renewable polysaccharide, easily available in nature with a high content of the functional group, low immunogenicity, large surface area for bio-conjugation, low manufacturing cost and has been used in biomedical areas in the form of sutures, wound healing materials and artificial skin [14, 15]. It has been widely studied in the preparation of nanoparticles for drug delivery [9, 16-23]. Due to the presence of amino group at the C-2 position of D-GlcN residues in the CS backbone, the polysaccharide is converted into polycation in acidic media [10, 18]. Therefore, micro and nanoparticles can be easily prepared by the electrostatic interactions between the amine groups of CS and a vaudeville of biocompatible polyanionic materials like fatty acids, citrate, sulfate, tripolyphosphate, etc. [18, 19, 22].

These interactions need unique moderate conditions in terms of temperature and pH [21, 22]. CS colloids are under immense studies mainly for several ways of delivery of many drugs (oral, vaginal, and parenteral) from a low molecular weight compounds to a heavy drugs), in order to improve the bioavailability of degradable substances such as proteins, or to enhance the uptake of hydrophilic substances across the epithelial layers [15, 20].

In the present study, myristoylated CS nanogel was prepared using myristate and loaded with SIL to produce MCS-SIL, and its loading was investigated. We focused on the characterization of the MCS nanogel beads by morphological observation and structural studies by scanning electron microscopy (SEM), Fourier-transform infrared (FT-IR) spectroscopy, and dynamic light scattering (DLS). Finally, anticancer effects of SIL and nano-SIL on cancerous and normal cells were also tested.

Materials and Methods

Chemicals and Reagents

CS, SIL, myristate, antibiotics (penicillin G, streptomycin and amphotericin B), 1-ethyl-3 (3-dimethylaminopropyl) Carbodiimide (EDC), N-hydroxysuccinimide (NHS) and 3-(4, 5-dimethylthiazol-2-yl) -2, 5-diphenyltetrazolium bromide (MTT) purchased from Sigma-Aldrich (USA). MCF-7 and human umbilical vein endothelial cells (HUVEC) cell lines were prepared from the Pasteur Institute of Iran (Pasteur Institute, Tehran, Iran). Dulbecco's Modified Eagle's Medium (DMEM), glutamine and fetal calf serum (FCS) were purchased from Invitrogen (Carlsbad, CA, USA). Glacial acetic acid, dimethyl sulfoxide (DMSO) and the other chemicals used in this research purchased of analytical grade from Merck (Germany).

Preparation of MCS Nanogel

MCS nanoparticles were prepared following the procedure described in our previous study [22] with some modifications. Briefly, 0.1g CS was dissolved in 20 ml of 1% acetic acid in distilled water (DW) with continuous stirring at room temperature (RT) to obtain 5mg/ml homogeneous viscous CS solution. The solution was sonicated with the power of 80W/ 15 min/ 25^{o}C. Five ml of 36mg EDC and 22 mg NHS in DW and 5 ml of 0.015g myristate in ethanol were added dropwise to the above mixture with continuous stirring and incubated for 30 min/ RT. Then, ethanol was added to the mixture. Stirring was continued for 2-5 hours. The solution was precipitated at pH=10 with 10N NaOH solution and then centrifuged at 6000g /15^{o}C/ 15min. The pellet was washed with ethanol and DW several times.

The precipitated gel was dissolved in acetic acid 2 %(v/v) and stored at 4^{o}C.

Nanogel Characterization

1. Particle Size

Particle size distributions were determined by SEM with the model of KYKY-EM3200 and Zeta Plus DLS with the model of Zeta Sizer Nano-ZS-90. The instrument determined Polydispersity Index (PDI). The replicates were more than 30. Prior to injecting the sample into the cuvette, the sample was sonicated to disperse the nanoparticles.

2. FT-IR Test

To demonstrate the formation of MCS nanogel, 100 mg from the CS, myristate, and MCS were separately ground thoroughly with KBr and tablets were prepared under a pressure of 600 kg/cm^2 using a hydraulic press. Afterward, the samples were characterized by a spectrophotometer of FT-IR with the model of Thermo Nicolet Nexus 870 FT-IR ESP (USA).

3. Dialysis-Based Drug Loading

Dialysis-based drug loading was determined using the method of Wang *et al*. [24]. About 0.5ml of SIL with 2mg/ml concentration was added to 2.0 mg/ml of MCS nanogel and incubated for 24h/ 4°C with shaking. To remove unloaded SIL, solutions were dialyzed using 3kDa MWCO dialysis bags against 30 ml phosphate-buffered saline /3 hours/37°C/pH 5.0. The loaded SIL was calculated.

4. Determination Loading Capacity (LC) and Loading Efficiency (LE) of SIL

The %LE and %LC of the SIL were calculated according to the following equations:

%LE = (Total amount of SIL − Free SIL) 100 / Total amount of SIL

%LC = (Total amount of SIL − Free SIL) 100 / Total Amount of MCS

Cell Culture and SIL Treatment

First, HUVEC and MCF-7 cell lines were floated in DMEM media with 10% FCS, 2mM glutamine, and a composition of antibiotics (consisted of penicillin G, 60 mg/L; streptomycin, 100 mg/L and amphotericin B, 50µL/L) were added and then were incubated in a humid and warm air (37°C, 5% CO_2, 95% air). For treating nano-SIL and SIL, sufficient amounts of the stock solution (1mg/ml in DMSO) of SIL were added into culture medium to achieve the indicated concentrations and then incubated with cells for 24h, whereas DMSO solution was used as a blank reagent.

Determination of Cell Viability

The viability of MCF-7 cell line was measured by MTT assay after treating nano-SIL

and SIL. Briefly, cells (10000/well) treateded with 0, 100, 150 and 200µg/ml of SIL and incubated for 24 hours. Then, cell washing with an isotonic phosphate buffered saline solution (PBS) were done twice and 0.5 mg/mL MTT was added to each well and maintained under the temperature of 37°C for 3h. The crystals of formazan were created and dissolved in 100 µL/ well DMSO. Then the absorbance was read at 570 nm by an ELISA reader (Organon Teknika, Netherlands). The amount of toxicity was measured by the formula below:

$$\text{Cytotoxicity\%} = 1 - \frac{\text{Mean absorbance of toxicant}}{\text{Mean absorbance of negative control}} \times 100$$

To decrease the probability of error, the absorbance of some wells containing MTT stain alone and without cells were measured. Finally, the obtained amount was subtracted from the total other absorbance.

IC50 Determination

IC50 quantity for nano-SIL treating on MCF-7 and HUVEC cell lines were calculated after 24h. IC50 was distinguished by using probit analysis, the Pharm PCS (Pharmacologic Calculation System) statistical package (Springer- Verlag, USA)

Statistical Analysis

Data were analyzed by SPPS-19 using Student's t-test and one-way variance. The significant level was set at $P < 0.05$

Results

CS Nanogels and Particle Size

According to the Figure-1 and Table-1, the average diameter of the MCS nanogels which characterized by SEM was of about 20nm.

Table 1. SEM and DLS of MCS Nanogels. A mixture of Myristate: CS at a Ratio of 1:9.

MCS	S1
Mean Particle size by SEM	20.38
DLS Record Number	30
Zeta potential (mV)*	18.7± 3.02
Z-Average size (d. nm)*	20.46 ± 4.07
PDI	0.084

* Data presented as mean±SD

The Zeta potential of the nanoparticles determined in PBS /25°C are given in Table-1 and Figure-2. The average size of the particles obtained by Zeta-potential was of about 18nm (Figure-2a). The size distribution was found to be 20nm (Figure-2b). The polydispersity obtained was about 0.08. The SEM image also confirmed the spherical and dense surface with a homogeneous matrix. The best myristate: CS ratio was found to be 1:7 till 1:9.

In vitro Drug Loading

The results of drug loading are shown in Table-2. Incubation time up to 24h enhanced the loading efficiency of SIL up to about 95%. The drug loading partially increased with increasing MCS concentration to obtain 1:1 ratio of SIL: MCS.

FT-IR Analysis

The structural characterizations of non-modified CS, myristate, and MCS evaluated with FT-IR spectrometry is shown in Figure-3. From the obtained peaks in non-modified CS (Figure-3a), the non-sharp characteristic peak and a very strong broad peak have seen at 2867 cm^{-1} and 3367 cm^{-1}, respectively. The absorption band at 1075 cm^{-1}, 1550 cm^{-1}, 1647 2158 cm^{-1} and 3390 cm-1 have been observed in the MCS (Figure-3c).

Nano-SIL Cytotoxicity

Cytotoxicity effects of several concentrations of SIL and nano-SIL during 24h have been evaluated on MCF-7 and HUVEC cell lines. Production of MCF-7 cells was significantly inhibited by of SIL and nano-SIL in a concentration-related manner in 24 h ($P<0.05$). The relative number of the viable cells after treatment with different concentrations of SIL and nano-SIL determined by MTT assay is shown in Figure-4.

IC50 Determination

Proliferation of MCF-7 cells was significantly prevented by SIL and nano-SIL under a concentration- related manner in defining times ($P<0.05$). There was specific variation in IC50 SIL and nano-SIL ($P<0.01$). Compared to SIL alone($P<0.05$), SIL was more effective when it was loaded in nanogels ($P<0.01$).

Table 2. Drug Loading of MCS-SIL

SIL (mg/ml)	MCS:SIL	Loading Capacity (SIL/mg MCS)	Drug Loaded (mg/L)	Loading Efficiency (%)
2	1:1	88.3	4413	85.3- 95.2

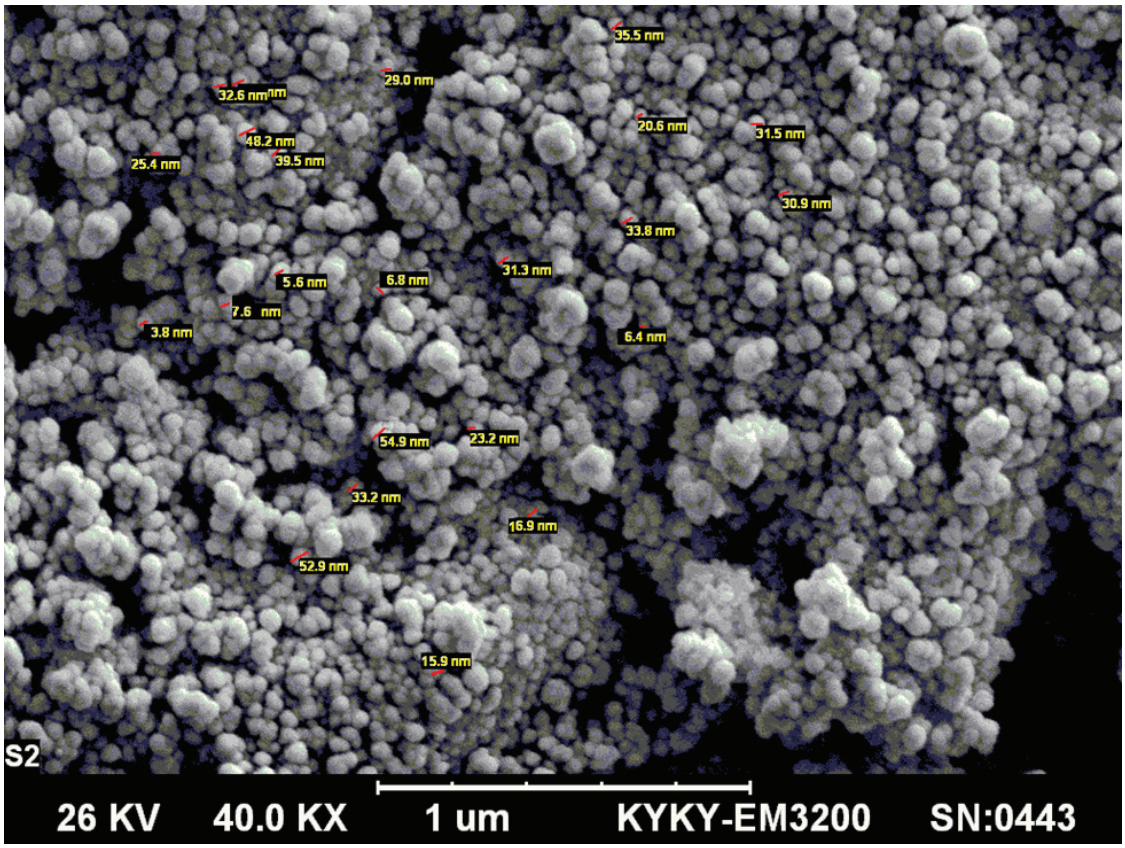

Figure 1. SEM of MCS nanogels.

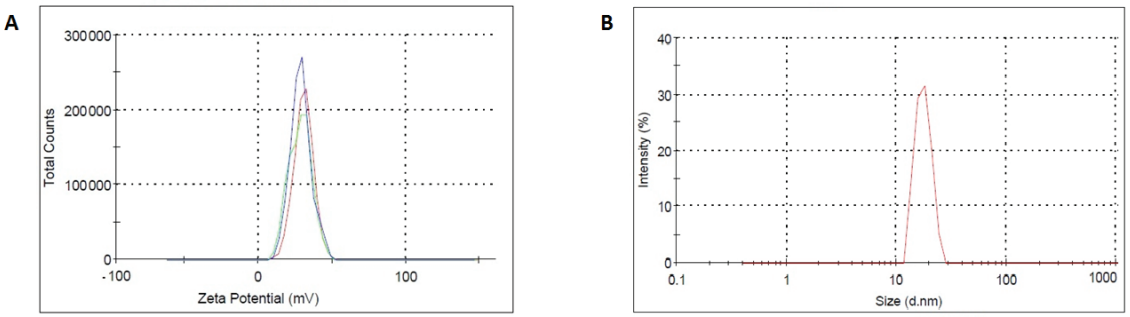

Figure 2. DLS results for MCS nanogels. **(A)** Zeta potential distribution; **(B)** Size distribution report by intensity.

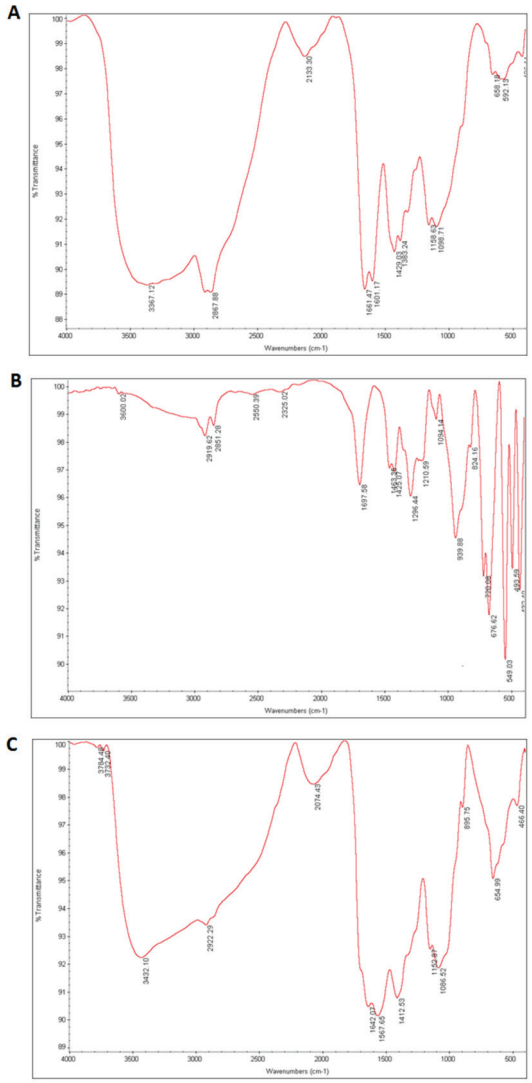

Figure 3. FTIR spectra of CS **(A)**, myristate **(B)** and MCS **(C)**.

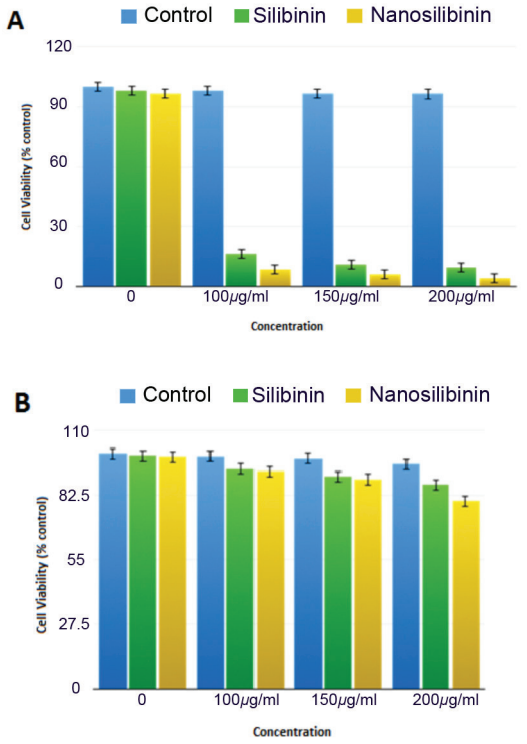

Figure 4. The relative number of the viable MCF-7 and HUVEC cells after treatment of different concentrations of sil was determined by mtt assay. **A:**MCF7 cell line; **B:**HUVEC cell line

The IC50 of SIL and SIL-nanogel for the MCF-7 cell line /24h was evaluated 15.771 µg/ml and 7.914 µg/ml, respectively ($P<0.01$). The effect of SIL obtained a significant variation on MCF-7 and HUVEC cell lines degradation ($P<0.01$).

Discussion

CS is considered to be a non-toxic [5, 25], biocompatible, with the reactive sites, the hydroxyl and amino groups of glucosamine units, for crosslinking reactions. [24-27]
Following treatment makes MCS nano drug, the positive charge of CS makes a strong electrostatic interaction with a negatively charged mucosal surface, making it a suitable drug-delivery system for the selective delivery. The micro and nanoparticle size can be controlled by changing the CS: myristate ratio, pH and their molar mass [23, 26, 27].
CS concentration also plays a crucial role in the particle size and Tsai *et al*. demonstrated that increasing CS concentration could result increasing the mean diameter of nanoparticles [23]. The CS concentration used in our study was 5 mg/ml, and the small particle size can be attributed to the low concentration of CS.
The conventional methods (operation, biochemical drug therapy, and radiation) for the treatment of different cancers have a lethal effect on healthy cells, as well as the cancerous tissues [28,29].
There is a desirable idea in preventing the carcinogenesis. So using vegetables, specified fruits, and grains, plus other phytotherapeutic materials with a favorable anticancer effect and less toxic effect on normal tissues have been a favorable daily habit.

SIL is such a dietary agent with numerous pharmacological properties.

Preventing DNA synthesis, cell production and differentiation inhibition, cell cycle and apoptosis development in various cancerous cell lines including breast cancer are a part of SIL capabilities. Moreover, this material in many studies has been known to be nonpoisonous in various animals [13].

The existence of an important prevention of cell growth and DNA synthesis has been shown after treating SIL on some cancerous cells, like prostatic cells, mammalian and cervical cancerous cells in a time-related manner. In 2011, Entezari *et al*. found the inducing effect of SIL on apoptosis and death progression in MCF-7 cells [1].

So preventing angiogenesis and anti-angiogenic therapy are mentioned as efficient strategies for controlling the metastasis and the growth of solid benign and malignant tumors in addition to the other disease related to the pathological angiogenesis.

Singh *et al*. (2009) showed the pleiotropic anti-angiogenic effect of SIL in human endothelial cells. They also showed; (a) the inhibition effect of SIL on capillary tube formation on matrigel; (b) outage of the capillary network; (c) inhibition of matrigel invasion and immigration; and (d) inhibition of MMP-2 secretion by HUVEC. In brief, some pleiotropic anti-angiogenic effects of SIL involve inhibition of growth, arresting the cell cycle, induction of apoptosis, prevention of capillary tube formation, reduction of invasion and migration of human endothelial cells [2]. In this research, we showed the inhibitory effect of SIL with a dose-related effect on the survival of MCF-7 and HUVEC cell lines.

The drug loading capacity was increased with increasing drug concentration [22]. The 24h incubation time enhanced the loading efficiency of SIL up to 95%.

At the constant amounts of SIL, the drug loading partially increased with increasing MCS concentration to obtain 1:1 ratio of SIL: MCS. Jayakumar *et al*. [25] obtained the loading efficiency of about 26% in Chitin drug within 5h.

They reported that the only factor affecting the loading efficiency is increasing the incubation time.

However, the size of the Chitin loaded drug nanogels remained constant because of the surface absorption of the drug [25].

Taranejoo *et al*. [30] demonstrated that other factors such as the concentration of CS and the amount of tripolyphosphate (TPP), drug polymer ratio and stirring speed might affect the loading efficiency of drug or biological agents in MCS. Shahsavari *et al*. [31] also reported that decreases in the concentration ratio of CS/TPP consequently cause an increase in entrapment efficiency. Slow release of drug molecules out in an aqueous phase from polymeric conjuncts, could provide a continuous release of drug out in the tumoral tissue [22]. This sustained release of drug at the target site would take an additional advantage in decreasing the tumor volume [32].

The peak at 1601 cm^{-1} could be attributed to N-H bending, at 1158 cm^{-1} belongs to C–O–C in glycosylic linkage and 1661 cm^{-1} is due to C=O carbonyl stretching vibrations of the esteemed group in CS.

The non-sharp characteristic peak at 2867 cm^{-1} is due to the C–H stretching vibrations of methyl or methylene group. The stretching vibration of the O-H group is overlapped to the N-H stretching band at 3367 cm^{-1} to give a very strong and broad peak in non-modified CS. Similar results were also reported by Mitra *et al*. [33].

The peaks at 592 cm^{-1} and 658 cm^{-1} are because of O–C–O scissors present in CS structure. Following the chemical modification of CS, the absorption band at 1601 cm^{-1} is moved to a lower position at 1550 cm^{-1} after MCS formation, and 1661 cm^{-1} is shifted to 1647 cm^{-1} in the MCS.

The absorption band at 2133 cm^{-1} in CS is shifted to 2158 cm^{-1} in MCS.

The C–O stretching absorption peak of the secondary hydroxyl group at 1098 cm^{-1} in CS became stronger and was shifted to 1075 cm^{-1} in the MCS. The characteristic peaks from the N–H stretching band and the O–H stretching band are overlapping at 3390 cm-1 in the MCS and at 3367 cm^{-1} in CS were also confirmed by FT-IR spectroscopy.

Conclusion

Our simple MCS-SIL formulation can be replaced with complicated procedures used for the preparation of the same kind. Availability, non-toxicity, biodegradability, biocompatibility and low immunogenicity of the renewable polysaccharide, i.e, CS are attractive features of this nanoparticle for drug delivery. High loading capacity with a low releasing slope of SIL from MCS suggests that MCS nanogels could be an alternative career as a cancer therapeutic agent.

Acknowledgments

I would like to thank of Tehran medical sciences branch, Islamic Azad University, Tehran, Iran

Conflict of Interest

The authors report no conflict of interests.

References

1. Entezari M, Mokhtari MJ, Hashemi M. Evaluation of Silibinin on the Viability of MCF-7 Human Breast Adenocarcinoma and HUVEC (Human Umbilical Vein Endothelial) cell lines. Advanced Studies in Biology. 2011;3(6):283-8.
2. Singh RP, Raina K, Sharma G, Agarwal R. Silibinin inhibits established prostate tumor growth, progression, invasion, and metastasis and suppresses tumor angiogenesis and epithelial-mesenchymal transition in transgenic adenocarcinoma of the mouse prostate model mice. Clin Canc Res. 2009; (14): 7773-80.
3. Bravo-Osuna I, Vauthier C, Chacun H, Ponchel G. Specific permeability modulation of intestinal paracellular pathway by Chitosan -poly (isobutylcyanoacrylate) core-shell nanoparticles. Eur J Pharm Biopharm. 2008; (69):436-44.
4. Rees M, Moghimi SM. Nanotechnology: From fundamental concepts to clinical applications for healthy aging. Maturitas. 2012; 73(1):1-4. Elsevier.
5. Sonia TA, Sharma CP. Chitosan and its derivatives for drug delivery perspective. In: AnonymousChitosan for Biomaterials I Adv Polym Sci. 2011; (243): 23-53.Springer.
6. Raj L, Chauhan GS, Azmi W, Ahn JH, Manu J. Kinetics study of invertase covalently linked to a new functional nanogel. Bioresour Technol. 2011; (102): 2177-84.
7. Hoare T, Sivakumaran D, Stefanescu CF, Lawlor MW, Kohane DS. Nanogel scavengers for drugs: Local anesthetic uptake by thermoresponsive nanogels. Acta Biomat. 2012; (8): 1450-58.
8. Yang X, Zhang X, Liu Z, Ma Y, Huang Y, Chen Y. High-efficiency loading and controlled release of doxorubicin hydrochloride on graphene oxide. J Physical Chem. 2008; (112): 17554-8.
9. Morris GA, Castile J, Smith A, Adams GG, Harding SE. The effect of prolonged storage at different temperatures on the particle size distribution of tripolyphosphate (TPP)-Chitosan nanoparticles. Carbohydr Polym. 2011; (84): 1430-4.
10. Kim YT, Yum S, Heo JS, Kim W, Jung Y, Kim YM. Dithiocarbamate Chitosan as a potential polymeric matrix for controlled drug release. Drug Dev Ind Pharm. 2013; (40):192-200.
11. Rinaudo M. Chitin and Chitosan : properties and applications. Prog Polymer Sci. 2006; (31): 603-32.
12. Bresolin JÑR, Largura MC, Dalri CC, Hoffer Gr, Rodrigues CvA, Lucinda-Silva RM. Spray-dried O-carboxymethyl Chitosan as potential hydrophilic matrix tablet for sustained release of drug. Drug Dev Ind Pharm. 2013; (40): 503-10.
13. Singla N, Sharma R, Bhardwaj TR. Design, Synthesis and In-Vitro Evaluation of Polymer-linked Prodrug of Methotrexate for the Targeted Delivery to the Colon. Lett Drug Des Discov. 2014; (11): 601-10.
14. Win PP, Shin-Ya Y, Hong KJ, Kajiuchi T. Formulation and characterization of pH sensitive drug carrier based on phosphorylated Chitosan (PCS). Carbohydr. Polym. 2003; (53): 305-10.

15. Rossi S, Ferrari F, Bonferoni MC, Sandri G, Faccendini A, Puccio A, et al. Comparison of poloxamer-and Chitosan -based thermally sensitive gels for the treatment of vaginal mucositis. Drug Dev Ind Pharm. 2013; (40): 352-60
16. Aranaz I, Harris R, Heras A. Chitosan amphiphilic derivatives. Chemistry and applications. Curr Organic Chem. 2010; (14): 308.
17. Anitha A, Deepa N, Chennazhi KP, Nair SV, Tamura H, Jayakumar R. Development of mucoadhesive thiolated Chitosan nanoparticles for biomedical applications. Carbohydr Polym. 2011; (83): 66-73.
18. Morris GA, Kok SM, Harding SE, Adams GG. Polysaccharide drug delivery systems based on pectin and Chitosan. Biotechn Genet Engin Rev. 2010; 27:257-84.
19. Tsai ML, Chen RH, Bai SW, Chen WY. The storage stability of Chitosan / tripolyphosphate nanoparticles in a phosphate buffer. Carbohydr Polym. 2011; (84): 756-61.
20. Arias JÑL, Martonez-Soler GI, Lopez-Viota M, Ruiz MÒA. Formulation of Chitosan nanoparticles loaded with metronidazole for the treatment of infectious diseases. Lett Drug Des Discov. 2010; (7): 70-8.
21. Zhang H, Oh M, Allen C, Kumacheva E. Monodisperse Chitosan nanoparticles for mucosal drug delivery. Biomacromolecules. 2004; (5): 2461-8.
22. Atabi F, Gargari SLM, Hashemi M, Yaghmaei P. Doxorubicin Loaded DNA Aptamer Linked Myristilated Chitosan Nanogel for Targeted Drug Delivery to Prostate Cancer. IJPR. 2017; 16(1): 35-49.
23. Tsai ML, Bai SW, Chen RH. Cavitation effects versus stretch effects resulted in different size and polydispersity of ionotropic gelation Chitosan GÇôsodium tripolyphosphate nanoparticle. Carbohydr Polym. 2008; (71): 448-57.
24. Wang C, Mallela J, Garapati US, Ravi S, Chinnasamy V, Girard Y, et al. A Chitosan -modified graphene nanogel for noninvasive controlled drug release. Nanomedicine: Nanotech Bio Med. 2013 (9): 903-11.
25. Jayakumar R, Nair A, Rejinold NS, Maya S, Nair SV. Doxorubicin-loaded pH-responsive chitin nanogels for drug delivery to cancer cells. Carbohyd Polym. 2012; (87): 2352-6.
26. Ibezim EC, Andrade CT, Marcia C, Barretto B, Odimegwu DC, de Lima FF. Ionically Cross-linked Chitosan /Tripolyphosphate Microparticles for the Controlled Delivery of Pyrimethamine. Ibnosina J Med Biomed Sci. 2011 (3).
27. Xu X, Chen X, Ma PÂ, Wang X, Jing X. The release behavior of doxorubicin hydrochloride from medicated fibers prepared by emulsion-electrospinning. Eur J Pharm Biopharm. 2008; (70): 165-70.
28. Bakhshayesh M, Zaker F, Hashemi M, Katebi M, Solaimani M. TGF- β1-mediated apoptosis associated with SMAD-dependent mitochondrial Bcl-2 expression. Clin Lymphoma Myeloma Leuk. 2012;12(2):138-43.
29. Saliani N, Darabi M, Yousefi B, Baradaran B, Khaniani MS, Darabi M, et al. PPARγ agonist-induced alterations in Δ6-desaturase and stearoyl-CoA desaturase 1: Role of MEK/ERK1/2 pathway. World J Hepatol. 2013;5(4):220-5.
30. Taranejoo S, Janmaleki M, Rafienia M, Kamali M, Mansouri M. Chitosan microparticles loaded with exotoxin A subunit antigen for intranasal vaccination against Pseudomonas aeruginosa: An in vitro study. Carbohyd Polym. 2011;1861(83): 1854-61.
31. Shahsavari S, Vasheghani-Farahani E, Ardjmand M, Abedin Dorkoosh F. Modeling of Drug Released from Acyclovir Nanoparticles Based on Artificial Neural Networks. Lett Drug Des Discov. 2014; (11): 174-83.
32. Cao Y, Gu Y, Liu L, Yang Y, Zhao P, Su P, et al. Reversion of multidrug resistance using self-organized nanoparticles holding both doxorubicin and targeting moiety. Lett Drug Des Discov. 2010; (7): 500-6.
33. Mitra T, Sailakshmi G, Gnanamani A, Mandal AB. Studies on Cross-linking of succinic acid with Chitosan /collagen. Mat Res. 2013; (16): 755-65.